Solar cell with built-in charge: Experimental studies of diode model parameters

Kimberly A. Sablon[a] and John W. Little
U.S. Army Research Laboratory, 2800 Powder Mill Road, Adelphi, Maryland 20783

Andrei Sergeev, Nizami Vagidov, and Vladimir Mitin
University at Buffalo, State University of New York, Buffalo, New York 14260

(Received 12 January 2012; accepted 27 March 2012; published 19 April 2012)

Quantum dots acquire built-in charge due to selective *n*-doping of the interdot space. The **q**uantum dots with **b**uilt-**i**n **c**harge (Q-BIC) increase electron coupling to IR radiation and suppress photoelectron capture, which in turn decrease the recombination via quantum dots. To investigate effects of the built-in-dot charge on recombination processes and device performance, the light and dark *I–V* characteristics and their temperature dependences of Q-BIC solar cells are measured. Employing the diode model, the data are analyzed in terms of the ideality factor, shunt resistance, and reverse saturation current. The authors compare the *n*-doped Q-BIC solar cells with the GaAs *p-i-n* reference cell, undoped, and *p*-doped devices. The analysis provides a qualitative description of the effect of doping on carrier kinetics and transport. The authors show that *n*-doping substantially reduces the recombination via quantum dots. © *2012 American Vacuum Society*. [http://dx.doi.org/10.1116/1.3703607]

I. INTRODUCTION

Quantum dots (QDs) have attracted much attention for applications in the third generation solar cells due their ability to harvest IR radiation, which is expected to increase the photovoltaic conversion efficiency.[1–4] However, the increased recombination losses limit the usage of QD layers in solar cells.[5–8] Although several studies have demonstrated some improvements in the short-circuit current, I_{SC}, due to absorption of longer wavelength photons, this increase was usually accompanied by deterioration of the open-circuit voltage, V_{OC}. As a result, the improvement in conversion efficiency did not exceed a few percent.[5–8]

Our novel approach to the optimization of photocarrier kinetics for effective photovoltaic conversion is based on quantum dots with built-in charge (Q-BIC). We demonstrated[9–11] that the Q-BIC medium provides strong coupling to IR radiation and long photocarrier lifetimes. The Q-BIC solar cells show significant (up to 60%) improvements in I_{SC} without deterioration of V_{OC}. To further understand the effect of the built-in-dot charge on electron processes, we performed a detailed study of the temperature and doping dependences of the light and dark *I–V* characteristics of *n*-doped, *p*-doped, and undoped QD solar cells as well as a GaAs *p-i-n* reference cell.

II. EXPERIMENT

The studied structures were grown on n^+ GaAs (100) substrates by molecular beam epitaxy. The *n*- and *p*-doped Q-BIC structures consist of a plane of dopants placed in the middle of each GaAs layer that separates the QD layers. The average lateral size of the InAs QDs was 30 nm and the average height about 3.6 nm. The sheet density of the QDs was about 1.2×10^{10} cm^{-2}. The structures contained 20 stacks of InAs QD layers separated by GaAs with various dopant sheet densities providing zero, two, three, four, and six electrons per dot (see Fig. 1). The thickness of the GaAs layers (50 nm) was chosen substantial enough to dissipate strain fields in the subsequent layers and to minimize strain accumulation in multistack samples.

Further details of the growth and fabrication processes have been described elsewhere.[9] The current–voltage characteristics of our devices were measured under light from a Newport Oriel PV calibrated solar simulator, which provides 1 Sun (AM1.5G) illumination. Solar cell parameters such as I_{SC}, V_{OC}, fill factor (FF), and cell efficiency have been obtained from the resulting curves. In order to examine carrier transport mechanisms, the temperature-dependent dark *I–V* characteristics were measured using a thermoelectric Peltier cooler/heater connected to a Hewlett-Packard 6651A power supply. A temperature probe was used for monitoring the temperature in the range of 296–400 K. The data obtained were analyzed in the framework of the diode model in terms of the ideality factor, *n*, diode saturation current, I_0, and the shunt resistance, R_{SH}.

III. RESULTS AND DISCUSSION

The dependences of the Q-BIC solar cell efficiency on the magnitude of the built-in-dot charge (doping) are summarized in Fig. 2. Figure 2 shows a strong enhancement of conversion efficiency of the *n*-doped devices without deterioration of the open-circuit voltage. As seen, the maximum of the efficiency increases from 9% for the reference cell or the undoped QD cell to 14% for Q-BIC solar cell with the built-in charge of six electrons per dot. In contrast to the positive effect of *n*-doping, the *p*-doping deteriorates the solar cell performance. The QD solar cell with the built-in charge of four holes per dot shows a maximum efficiency of 8%. These dependences can be attributed to the fact that the capture processes of photoelectrons into the QDs are

[a]Electronic mail: kimberly.a.sablonramsey.civ@mail.mil

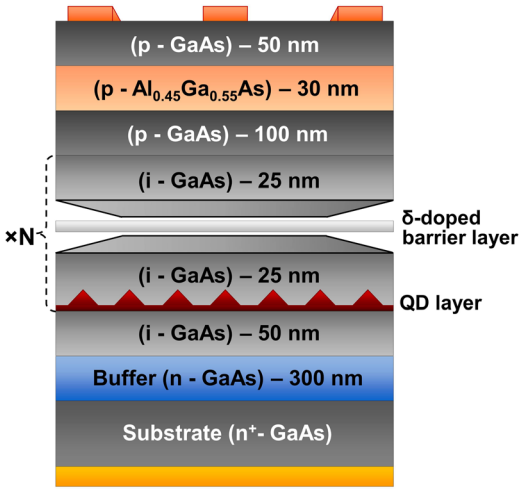

FIG. 1. (Color online) Schematic view of the solar cell with quantum-dot layers.

substantially faster than the corresponding processes for holes.[9–11] To decrease recombination via QDs, one should suppress the fast capture processes, i.e., capture of photoelectrons. Keeping in mind that a negative built-in-dot charge prevents capture of electrons, we expect that the *n*-doping will decrease the recombination losses, while *p*-doping will increase these losses.

To further understand the electron processes, we investigate the temperature and doping dependences of the dark *I–V* characteristics. Figure 3 shows the semilogarithmic plot of the *I–V* characteristics measured in the range of 296–380 K for the *p*-doped sample [Fig. 3(a)] and *n*-doped sample [Fig. 3(b)] with the same doping level, which corresponds to four carriers per dot. The *I–V* curves of the GaAs *p-i-n* reference cell are shown in Fig. 3(c). As seen, the dark current in the *p*-doped sample is an order of magnitude higher than that in the *n*-doped sample. This evidences the strong enhancement of the recombination-generation processes in the *p*-doped sample.

To gain better understanding of the recombination processes and corresponding losses, we analyze the *I–V* characteristics in terms of the diode model.[12,13] The corresponding

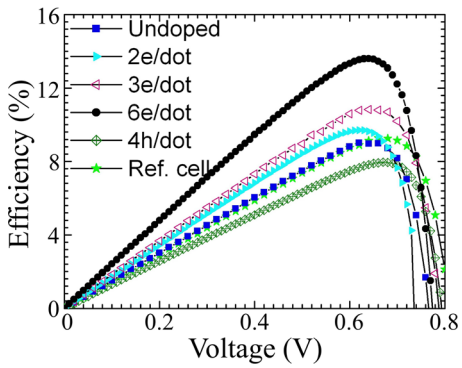

FIG. 2. (Color online) Solar cell conversion efficiency under 1 Sun (AM1.5G) solar irradiation as a function of the output voltage for *p*-doped QD cell with four holes per dot, GaAs *p-i-n* reference cell, undoped QD cell, and *n*-doped QD cells with two, three, and six electrons per dot.

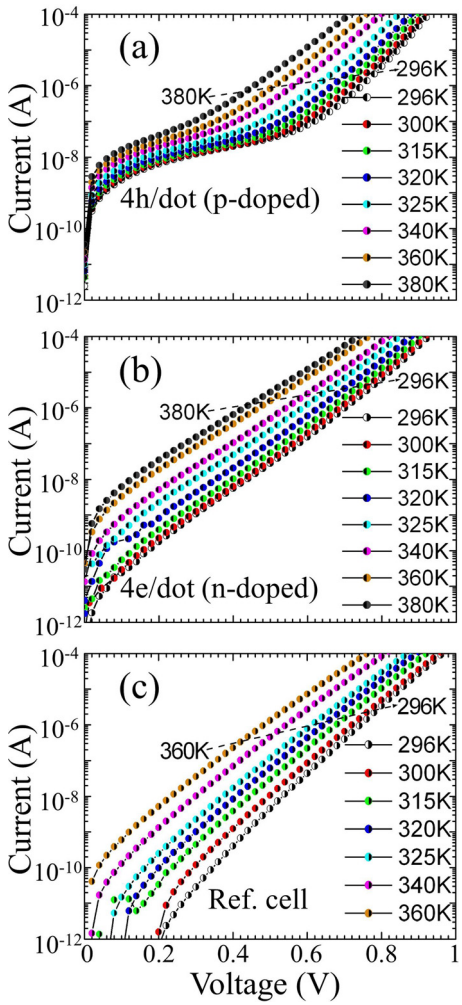

FIG. 3. (Color online) Dark *I–V* characteristics of (a) *p*-doped QD solar cell, (b) *n*-doped QD solar cell, and (c) GaAs *p-i-n* reference cell for a set of temperatures: 296, 300, 315, 320, 325, 340, 360, and 380 K.

equivalent circuit diagram shown in Fig. 4 includes the photocurrent source, the shunt resistance, R_{SH}, the series resistance, R_{SR}, and the diode, D, where the variety of recombination processes are taken into account by the ideality factor, *n*. In this model the *I–V* characteristics are described by

$$I = I_0\left(\exp\left(\frac{e(V - IR_{SR})}{n\,k_BT}\right) - 1\right) - I_{SC} + \frac{V - IR_{SR}}{R_{SH}}. \quad (1)$$

At high voltages, $V \gg k_BT/e = 25$ mV, the *I–V* curves are defined by the exponential term, from which the ideality factor, *n*, may be determined. The ideality factor is a characteristic of the generation-recombination (G-R) processes in the photovoltaic device. As it is known, $n = 1$ corresponds to the radiation processes in the charge-neutral regions and $n = 2$ or greater is associated with the recombination via midgap traps in the space-charge region (the Shockley–Read–Hall recombination). As we mentioned earlier, altogether with the IR radiation harvesting via QD levels, QDs also induce the G-R processes with subgap energies. For this reason, a QD solar cell, along with substantial conversion of subgap photons, has significant G-R processes via QDs and

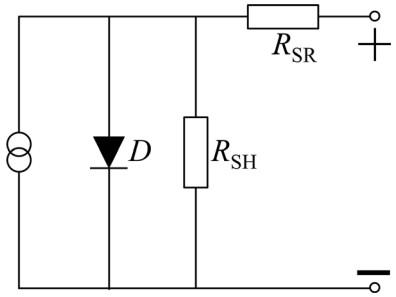

FIG. 4. Equivalent circuit diagram of the solar cell.

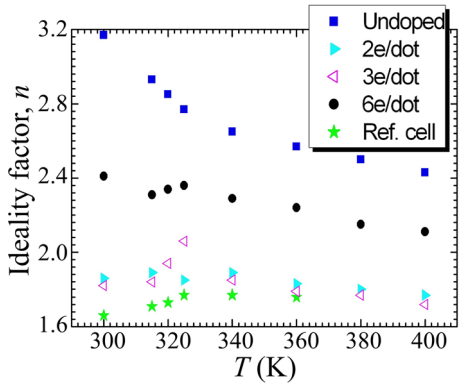

FIG. 5. (Color online) Temperature dependence of the ideality factor of the GaAs *p-i-n* reference cell, undoped QD cell, and *n*-doped QD cells with two, three, and six electrons per dot.

the ideality factor increases up to 3 or even more.[14] As the carrier capture and charge extraction from the QDs depend on the electric field, the intensity of the corresponding G-R processes and the ideality factor also depend on applied voltage.

According to the obtained data the *p*-doped sample as well as the undoped sample cannot be described by the curves with a single ideality factor, n. For the *p*-doped sample the ideality factor changes from $n \approx 5$ at low voltages to $n \approx 1.6$ at high voltages. For the undoped sample the ideality factor changes from $n \approx 3.2$ at low voltages to $n \approx 1.6$ at high voltages. The large values of n at low voltages and the dependence of n on output voltage evidence the strong recombination via QDs in these samples.

The temperature dependences of ideality factor are presented in Fig. 5. For the undoped QD solar cell the ideality factor decreases with temperature. In particular, the low-voltage ideality factor changes from 3.2 at 300 K to 2.4 at 400 K. Assuming that G-R processes via QDs dominate in this case,[14] this temperature dependence may be explained as follows. As discussed in Ref. 9, without doping the electron capture to QDs is substantially faster than the corresponding capture of holes. Therefore, the recombination in the QDs is determined by the capture rate of holes. At the same time, the energy level spacing for holes in the QDs is relatively small and comparable with the thermal energy. For this reason, hole capture consists of a number of thermal relaxation and excitation processes via the QD levels. The rate of such cascade capture decreases with temperature,[15] which leads to a decrease of the recombination processes via the QDs in favor of radiative recombination in the charge-neutral region.

The electron energy level spacing substantially exceeds the spacing for holes and the thermal energy. For this reason, it is precisely the electron intradot processes that limit the electron–hole escape from the QDs. Thus, it is critically important to enhance the photoexcitation of electrons rather than holes.

In contrast to the *p*-doped and undoped devices, the *I–V* curves of the *n*-doped solar cells are well described by a single exponent in the wide range of voltages. Figure 5 presents the temperature dependence of the ideality factor for *n*-doped QD solar cells, GaAs *p-i-n* reference cell, and the undoped QD solar cell. The ideality factor for the GaAs reference cell is practically temperature independent and is equal to $n \approx 1.7$, which is close to the values obtained in other works.[7] For the undoped QD solar cell, the ideality factor is $n \approx 3.2$ at 300 K and decreases to $n \approx 2.4$ when the temperature increases to 400 K. As we already discussed, such large values of n are a clear indication of strong G-R processes via the QDs. However, with the *n*-doping which provides two to four electrons per dot, the ideality factor decreases and varies in the range of 1.7–2. This observation is completely aligned with our main conclusion that the *n*-doping suppresses the recombination via dots.[9] For the *n*-doped solar cell with six electrons per dot, the ideality factor increases and shows weak temperature dependence, where it changes from $n \approx 2.4$ at 300 K to $n \approx 2.1$ at 400 K. While recombination via the QDs increases, the conversion efficiency of the *n*-doped solar cells with the QDs is enhanced due to increased IR harvesting. Note that in the *n*-doped QD solar cells the recombination via dots is substantially weaker than in the undoped QD solar cells.

In Fig. 6, we present the temperature dependences of the saturation diode current, I_0. As seen for all devices, I_0 shows an exponential temperature dependence, $I_0 = I_{00} \exp(-\Delta/k_B T)$. For the GaAs reference cell, the activation energy, Δ, determined from this plot is ~1.4 eV, which corresponds to the GaAs bandgap. When considering QD solar cells, let us note that the saturation current in the undoped QD solar cell is more

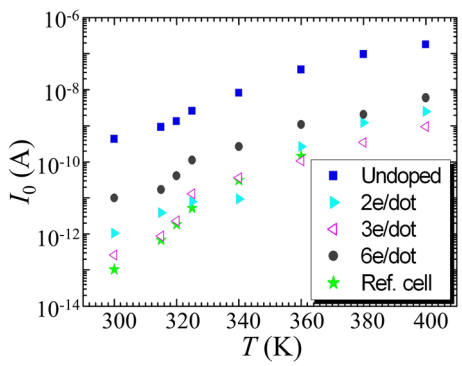

FIG. 6. (Color online) Temperature dependence of the saturation current of the GaAs *p-i-n* reference cell, undoped QD cell, and *n*-doped QD cells with two, three, and six electrons per dot.

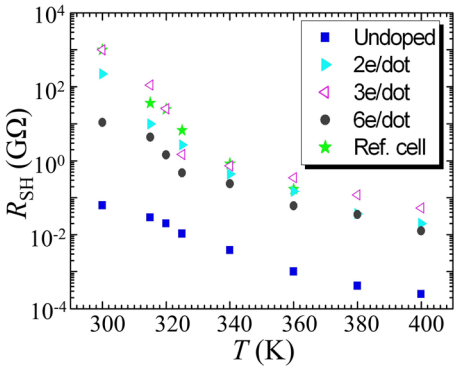

FIG. 7. (Color online) Temperature dependence of the shunt resistance, R_{SH}, of the GaAs *p-i-n* reference cell, undoped QD cell, and *n*-doped QD cells with two, three, and six electrons per dot.

than 2 orders of magnitude higher than that in the *n*-doped samples. At the same time, the activation energy weakly depends on doping and its value is in the range of 0.7–1 eV. As the activation energy in the diode model is given by the average energy of various electron transitions, weighted in accordance with their contributions to G-R processes, these data demonstrate that the G-R processes via QDs as well as in bulk GaAs contribute to the saturation diode current.

Figure 7 shows the temperature dependence of the shunt resistance, R_{SH}, which was determined from fitting the low-voltage part of the dark *I–V* curves of Eq. (1). The finite shunt decreases the filling factor, as

$$FF = FF_0[1 - V_{OC}/(I_{SC}R_{SH})], \quad (2)$$

where FF_0 is the filling factor at infinite shunt resistance. For the undoped QD solar cell the parameter $V_{OC}/(I_{SC}R_{SH})$ changes from 0.8 at 400 K to 0.002 at 300 K. Doping strongly improves the shunt resistance. For all *n*-doped devices even at 400 K the parameter $V_{OC}/(I_{SC}R_{SH})$ is below 0.01. Thus, in the entire temperature range, the losses due to shunt currents in the Q-BIC solar cells are below 1% of the output power.

IV. SUMMARY AND CONCLUSIONS

In this work, we have studied the effect of doping on the performance of the Q-BIC solar cells in terms of the ideality factor, shunt resistance, and reverse saturation current. We have found that *n*-doping significantly improves all the above-mentioned parameters, while *p*-doping leads to their deterioration. These observations are in agreement with our previous investigations of photoelectron kinetics based on photoluminescence experiments and spectral analysis of photoresponse.[9–11] The results of this work confirm that the negative built-in-dot charge suppresses the fast capture of thermally or photogenerated electrons into QDs and, thereby, decreases the recombination losses via QDs. Together with the enhanced electron coupling to IR radiation, these effects significantly improve the photovoltaic conversion efficiency of Q-BIC solar cells.

ACKNOWLEDGMENTS

This work was supported by the Air Force Office of Scientific Research (AFOSR). The authors thank Kimberley Olver for sample processing and Fred Towner of Maxion Technologies, Inc. for MBE growth.

[1]A. J. Nozik, Nano Lett. **10**, 2735 (2010).
[2]O. E. Semonin, J. M. Luther, S. Choi, H. Y. Chen, J. Gao, A. J. Nozik, and M. C. Beard, Science **334**, 1530 (2011).
[3]J. Gao, J. M. Luther, O. E. Semonin, R. J. Ellingson, A. J. Nozik, and M. C. Beard, Nano Lett. **11**, 1002 (2011).
[4]D. Guimard, R. Morihara, D. Bordel, K. Tanabe, Y. Wakayama, M. Nishioka, and Y. Arakawa, Appl. Phys. Lett. **96**, 203507 (2010).
[5]D. Zhou, P. E. Vullum, G. Sharma, S. F. Thomassen, R. Holmestad, T. W. Reenaas, and B. O. Fimland, Appl. Phys. Lett. **96**, 083108 (2010).
[6]R. Oshima, A. Takata, and Y. Okada, Appl. Phys. Lett. **93**, 083111 (2008).
[7]S. M. Hubbard, C. D. Cress, C. G. Bailey, R. P. Raffaelle, S. G. Bailey, and D. M. Wilt, Appl. Phys. Lett. **92**, 123512 (2008).
[8]A. Luque and A. Martí, Phys. Rev. Lett. **78**, 5014 (1997).
[9]K. A. Sablon, J. W. Little, V. Mitin, A. Sergeev, N. Vagidov, and K. Reinhardt, Nano Lett. **11**, 2311 (2011).
[10]K. A. Sablon, V. Mitin, A. Sergeev, J. W. Little, N. Vagidov, K. Reinhardt, and K. A. Olver, Proc. SPIE **8035**, 80350M (2011).
[11]K. A. Sablon, A. Sergeev, N. Vagidov, A. Antipov, J. Little, and V. Mitin, Nanoscale Res. Lett. **6**, 584 (2011).
[12]P. Würfel, *Physics of Solar Cells: From Basic Principles to Advanced Concepts* (Wiley-VCH, Weinheim, Germany, 2005).
[13]A. L. Fahrenbruch and R. H. Bube, *Fundamentals of Solar Cells: Photovoltaic Solar Energy Conversion* (Academic, New York, 1983).
[14]D. Di, I. Perez-Wurfl, A. Gentle, D-Ho Kim, X. Hao, L. Shi, G. Conibeer, and M. A. Green, Nanoscale Res. Lett. **5**, 1762 (2010).
[15]V. N. Abakumov, V. I. Perel, and I. N. *Yassievich*, *Nonradiative Recombination in Semiconductors* (Elsevier, Amsterdam, 1991).